# Observation of turbulent intermittency scaling with magnetic helicity in an experimental MHD plasma

D.A. Schaffner,[1] A. Wan,[1] and M.R. Brown[1]
*Swarthmore College, Swarthmore, PA, USA*

(Dated: 17 December 2013)

The intermittency in turbulent magnetic field fluctuations has been observed to scale with the amount of magnetic helicity injected into an experimental flux rope plasma. A selectively decayed Taylor state is created in the wind-tunnel configuration of the Swarthmore Spheromak Experiment using a magnetized plasma gun that can inject plasma of varying levels of helicity into the chamber. The level of intermittency is determined by finding the flatness of the probability distribution function of increments for magnetic pickup coil fluctuations, $\dot{B}(t)$. The intermittency is observed to increase with the injected helicity while the spectral index in the inertial range of the turbulence appears to be unaffected by this variation. Some experimental evidence is given for the role of current sheets and reconnection sites in the generation of this intermittency, but the true nature of the observed intermittency remains unknown.

Varying levels of intermittency[13] in magnetic fluctuations have been observed in many different turbulent plasmas in both space and laboratory settings. Differences in magnetic intermittent character have been seen between fast and slow solar wind turbulence[1], at varying spatial scales in the solar wind[14], and between different confinement regimes in laboratory experiments, particular in reverse field pinches[3,4]. Simulation generated intermittency in MHD turbulence[8–10,15] compared with *in situ* measurements in the solar wind has suggested a link between such non-Gaussian fluctuations and the presence of current sheets or reconnection layers. Since magnetic helicity of a plasma is reflective of the twistedness or knottedness of the magnetic field, a scan of magnetic helicity can be used in order to vary the magnetic field structure and consequently modify the character of current sheets in the plasma. A novel experiment was developed on the Swarthmore Spheromak Experiment (SSX) to explore this possible relationship between the observed intermittency in magnetic fluctuations and the magnetic helicity of the plasma. Given the nature of the plasma source on SSX, magnetic helicity injection can be very finely controlled and thus resulting changes in turbulent characteristics—including both spectra and intermittency—can be carefully examined.

This paper presents the results of an experimental scan which establishes a connection between a controllable experimental quantity—magnetic helicity—and a turbulent characteristic—intermittency. As the amount of injected magnetic helicity is increased, the measured flatness or kurtosis of the distribution of fluctuations in a magnetic pickup coil, $\dot{B}(t)$, are also shown to increase ranging from near Gaussian (F$\sim$ 5) to values of F ¿ 30. In contrast, the power-law behavior of the spectra of these fluctuations are shown to be unaffected by this variation in helicity as shown by the fit spectral indices. The scan is conducted on the wind-tunnel configuration of the Swarthmore Spheromak Experiment which consists of a 86cm long by 15.5cm wide cylindrical copper flux conserver into which a plasma gun injects dense, highly magnetized ($\sim 1 \times 10^{15} cm^{-3}, \sim 5kG$) plasma which self-organizes into a Taylor state[5]. There is no guide or vacuum field in the chamber so the magnetic field embedded in the plasma are completely dynamical.

The injection of magnetic helicity into the plasma is a natural consequence of the formation procedure for a plasma gun. Magnetic helicity,

$$K_B = \int A \cdot B dV \tag{1}$$

is a measure of the amount of twistedness of the magnetic field lines and can be expressed in terms of magnetic flux squared (i.e. units of $Wb^2$). This quantity can be recast in a more experimentally relevant quantity,

$$K_B = \int \Phi V_{gun} dt \tag{2}$$

where $\Phi$ is the magnetic flux penetrating the plasma gun core and $V_{gun}$ is the voltage drop across the gun gap. This is the form of the helicity that is calculated and reported as in this paper. Since the plasma forms under the assumption of selective decay (conservation of magnetic helicity) are reported in Gray 2013[5], it is further assumed that the amount of helicity injected by the gun is conserved and present in the plasma under observation. Though the voltage across the gun gap is recored for the entire duration of the shot, only the first $20\mu s$ are used to estimate the injected helicity. Beyond $20\mu s$, the voltage measurement is significantly affected by breaking fieldlines during spheromak formation. Though it is assumed that helicity injection is nearly constant for the duration of the discharge, the values of helicity reported here is that for the first $20\mu s$ after the initial trigger.

The gun voltage is set by a combination of the gun circuit and breakdown physics, but typically does not vary given a particular capacitor charge setting and gas input delay time. Thus, by 2, the injected helicity is modified by the amount of magnetic flux penetrating the gun core. This flux, in turn, is set by the the amount of current run through the stuffing coil. The stuffing coil produces magnetic field parallel to the gun axis using a capacitor

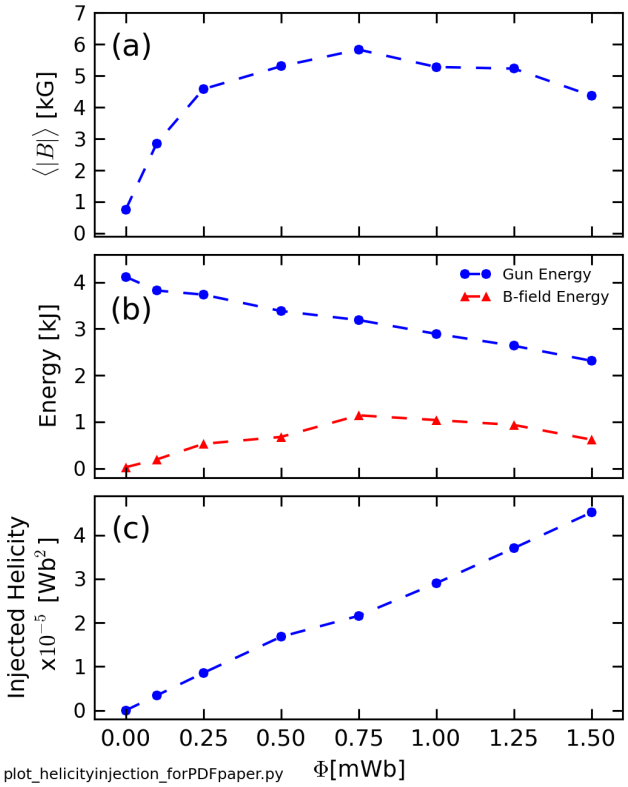


FIG. 1. (a) Average magnetic field magnitude over the equilibrium epoch (40-60$\mu s$), (b) injected gun energy and volume integrated magnetic field energy, and (c) amount of helicity injected in the first 20$\mu s$ after discharge trigger as a function of magnetic flux in gun core.

discharge circuit, but with a much longer timescale than the gun discharge. Because the stuffing coil discharge is much slower, rather than modify the discharge voltage to vary the magnetic field in the gun, the field is set by changing the timing of when the gun fires relative to the stuffing coil. Thus, changes in flux, and consequently helicity are adjusted by changing the timing delay of the gun trigger.

The flux can be ranged from 0.0 to 1.5mWb which, given a gun voltage of approximately 900V, yields an injected helicity range of 0 to $5x10^{-5}Wb^2$ for the first 20$\mu s$. As indicated in Figure 1(c), the injected helicity scales linearly with the varied magnetic flux. Figure 1(a) and (b) show how the average magnetic field in the center of the chamber and the energy changes with magnetic flux. The magnetic field is determined using a three-axis Bdot probe about 1cm off of the central cylindrical axis, and is time averaged from 40 to 60$\mu s$ which constitutes the equilibrium epoch of the discharge so called as it is the range of most time stationary fluctuations. As Figure 1(a) shows, this value increases initially with flux, but saturates at a value around $5kG$ for most flux settings. The gun energy is found by integrating the power, $P = I_{gun}V_{gun}$, from 0.0 to 60.0$\mu s$ and represents the maximum amount of energy that can be delivered into the plasma. This value begins around $4kJ$ which is about half of the possible circuit energy based on the 1mF, 4.0kV capacitor circuit, and decreases steadily with increasing flux as shown with blue in Fig. 1(b). The amount of energy that actually gets deposited into the magnetic fields is indicated by red in Fig. 1(b), and as would be expected, follows a similar trend as the field magnitude. This energy is calculated by finding the energy density, $B^2/2\mu_0$, for each Bdot tip, and integrating over the volume at each radially location.

Two turbulence analysis techniques, power spectra and probability distribution of increments are constructed using the magnetic pickup coil timeseries or $\dot{B}$ data. Since the probe is fabricated using a single 3mm wide loop, the $\dot{B}(t)$ signal has the best temporal resolution and bit-depth (65MHz sampling and 14-bit dynamic range) and is used directly in the analysis rather than converting the timeseries to $B(t)$ by integration. In frequency space, the $\dot{B}$ data can be scaled into B-field by dividing the power in each frequency bin by $f^2$. The PDF and flatness analysis uses $\dot{B}$ directly. The results shown are for a 20$\mu s$ period (40$to$60$\mu s$ after initial breakdown) during the plasma discharge that is in a quasi-stationary state between formation and decay of the plasma. Forty shots for each helicity state are taken to form an ensemble average of the turbulence measurements.

The power spectrum of magnetic field fluctuations for each helicity case is presented in Figure 2. The curves shown are constructed by taking the a sixth-order Morlet wavelet transform[11] of each $\dot{B}_r$ timeseries and scaled to $B_r$ by diving through by frequency squared. Each curve shows a cascade of power from low frequencies to high frequencies, though the absolute scale in Figure 2(a) has been artificially staggered in order to allow for each curve to be clearly seen. Each spectra exhibits a break-point at approximately 1MHz; a power-law fit with calculated error is made to the linear region around the break-point for each curve using a Maximum Likelihood Estimation method[12]. The spectral index and error for each fit is indicated in Figure 2. Though the helicity is increasing linearly, the power-law fit for each spectra does not change significantly, hovering around a slope of 3 for low frequency fits and around 5 for high frequency fits. This trend indicates that the change in helicity does not appear to have an effect on the cascade process from larger scales to smaller scales.

The amount of intermittency in the $\dot{B}(t)$ fluctuations for each helicity state does, however, appear to change. Figure 3 demonstrates how intermittency is determined through the measure of flatness. Fig. 3(a) shows the probability distribution function of increments (PDF) of a timeseries at $2\times10^{-5}$ Wb$^2$ of injected helicity for two different timescales: 0.15$\mu s$ and 15$\mu s$. The PDF of increments is constructed by taking differences of values in a time signal—in this case, $\dot{B}_r$—separated by a time scale. As Fig. 3(a) shows, the PDF with small time scale shows a highly pointed PDF with broad, fat tails indicating large excursions from the mean value—or intermittency. This non-Gaussian behavior is indicated by a

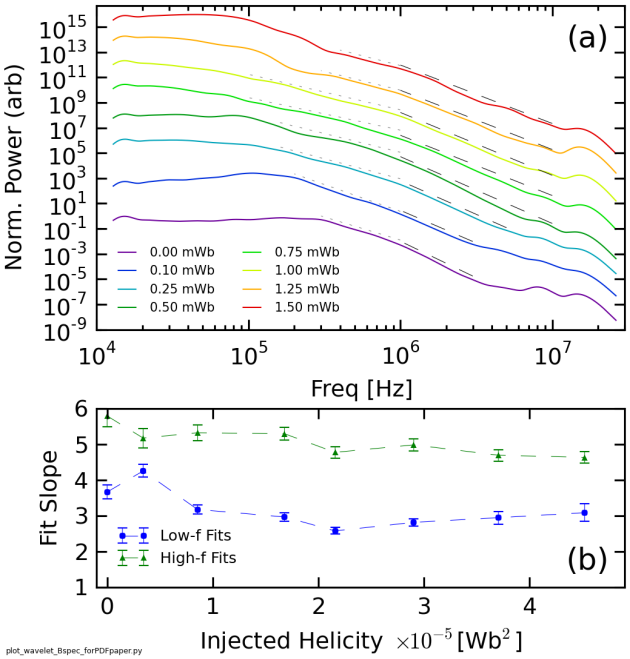


FIG. 2. (a) Wavelet generated magnetic field fluctuation spectra for the radial direction ($B_r$), for each of the eight helicity states. The spectra are staggered in order to highlight the shape of each spectrum. (b) Fits for each spectra for either low or high frequencies. The width in frequency of each fit is indicated by the dashed lines in (a).

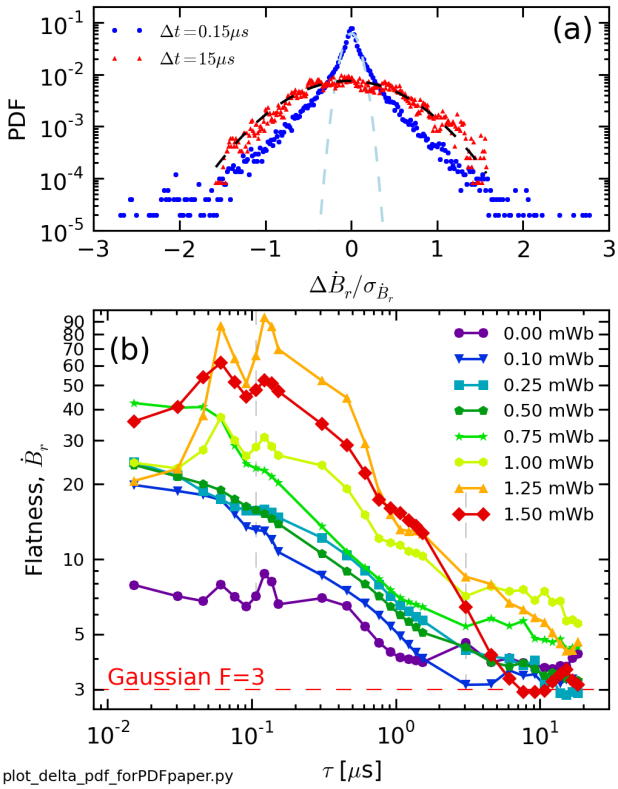


FIG. 3. (a) PDFs for a long and short $\tau$ from data for $K_B = 2 \times 10^{-5} Wb^2$ indicating the changing in intermittency with timescale. (b) Flatness values for each timescale and each helicity state for the radial $\dot{B}$ component.

best-fit Gaussian curve. The PDF with a large time scale increment clearly show a much more Gaussian distribution compared to its best fit. The level of intermittency for each scale can be quantified by taking the normalized fourth-order moment of the PDF—also called flatness or kurtosis. The flatness for each PDF at each times scale, as well as for each helicity state, is shown in Fig. 3(b). Clearly, each state shows increasing flatness, and thus intermittency, with decreasing time scale. The flatness of a purely Gaussian distribution is indicated at F=3. Moreover, it is observed that the overall flatness of each curve increases as a function of helicity. In other words, the intermittency of the plasma appears to increase with injected helicity.

This change with helicity is summarized in Figure 4(a) where the calculated flatness of each curve in Fig. 3(b) as well as those for $\dot{B}_\theta$ and $\dot{B}_z$ has been averaged between the scales indicated by the dashed gray lines: between $0.1\mu s$ and $3.0\mu s$, which approximately corresponds to a frequency range of 333kHz to 10MHz. The average flatness generally increases with helicity, although there is a brief reversal of trend at about $1\times10^{-5}$ Wb$^2$ before the curve begins to increase again.

While the physical origin of this observed intermittency and its trend with helicity is not completely understood in the context of this experiment, investigation of intermittency in space plasma yields some possible explanations. Simulations of MHD plasmas modeled after solar wind plasma with time series extracted in ways to match that of *in-situ* satellite observation[8?,9], have indicated a correlation between intermittency and the passing of current sheets or reconnection sites. Results on SSX suggest that the appearance and change in observed intermittency can be connected to the changing size and/or frequency of reconnection sites in the plasma. Since many past experiments on SSX have focused on observation of reconnection layers[16], the machine has a number diagnostics designed to measure signatures of reconnection. These diagnostics are a set soft X-ray photodiodes and the ion Doppler spectrometer (IDS) system. The soft X-ray diagnostics is designed to measure X-rays generated by fast tail electrons which were potentially accelerated in the electric field of reconnection cites. Meanwhile, the IDS can measure both burst of ion heating and flow also generated by reconnection events. Fig. 4(b-d) shows the output of these diagnostics for the same helicity scan limited to the same time range as the turbulence data presented above. Soft X-ray measurement shows an initial increase in x-ray light going from zero to small amounts of helicity, but then a consistent decrease in radiation from then on. Fig. 4 shows flatness of the ion temperature timeseries as a function of helicity constructed from increment PDFs with a timescale of $1\mu s$, the minimum timestep available for the IDS system. Like, the flatness curve of $\dot{B}$, the ion curve also increases with helicity. Meanwhile, the average measured ion tem-

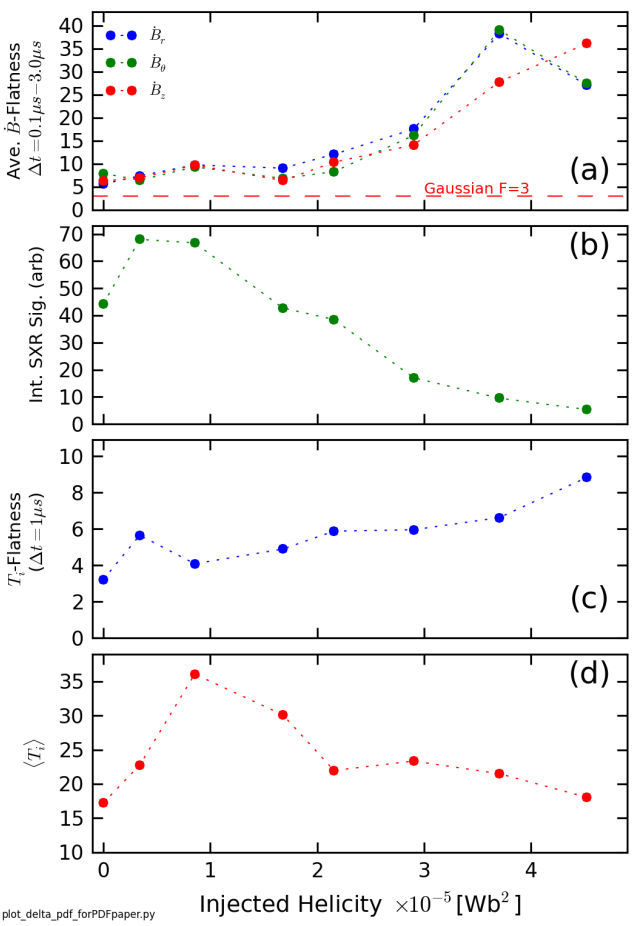


FIG. 4. (a) Average flatness versus helicity. (b) Integrated soft X-ray signal versus helicity. (c) Flatness of $T_i$ time series versus helicity. (d) Average $T_i$ versus helicity.

perature with flatness does not change too much, peaking slightly between 1 and $2\times10^{-5}$ Wb$^2$, but generally maintaining a value of between 20-25eV. Though all of these results are somewhat circumstantial, they all fit with the hypothesis of a changing reconnection site size. The decrease in soft X-ray may perhaps be due to decreasing reconnection size as electrons cannot be accelerated to as large as velocities with smaller sites. The increase in ion temperature bursts with little change in the mean ion temperature can arise from a high frequency of reconnection sites. Unlike electrons, the outflow velocity of ions is less likely to be modified by the physical size of the reconnection site.

Unfortunately, since the reconnection diagnostics used here measure line averaged quantities, better evidence for the affect of helicity on reconnection event size cannot be determined as of yet. However, as in solar wind experiments, comparison to simulation may help and studies using the HiFi simulation are underway.

This paper presents the observation of a clear change in intermittency as a function of injected helicity while simultaneously showing little to no change in the energy transfer rate between scales as indicated by the turbulent power spectra. This discrepancy is perhaps an indication of the need to study higher order moments in turbulence analysis (i.e. 4th order Flatness vs 2nd order spectra) in order to fully flesh out modifications in turbulence[20]. The experiment also demonstrates a straightforward method for modifying the intermittency in a plasma for detailed study. Finally, a possible connection to a physical mechanism was established through soft X-ray and IDS measurements, which suggested the intermittency is related to the spatial size of reconnection sites in the plasma. However, given the limitations of the current diagnostics, any definitive conclusions could not be made, but does provide impetus for further comparison to simulation.

Furthermore, since helicity observations have been made in many of the same turbulent plasmas mentioned previously[17–19], a link between helicity and turbulent intermittency may be a useful metric for understanding turbulence in these areas and future laboratory MHD experiments For example, the scaling can also be compared to variation of intermittency as a function of development time—perhaps the amount of helicity is connected to the age of the solar wind[21]?

## ACKNOWLEDGEMENTS

## REFERENCES

[1]Sorriso-Valvo, L. *et al.* Geophys. Res. Lett. **26**, 18011804 (1999).
[2]Wan, M. *et al.* ApJ. **744** 177 (2012).
[3]Sorriso-Valvo, L. *et al.* Planet. Space Sci. **49**, 11931200 (2001).
[4]Marrelli, L. *et al.* Phys. Plasmas. **12**, 030701 (2005).
[5]T. Gray, M. R. Brown, and D. Dandurand, Observation of a Relaxed Plasma State in a Quasi-Infinite Cylinder, Phys. Rev. Lett. **110**, 085002 (2013).
[6]J. B. Taylor, Rev. Mod. Phys. **58**, 741 (1986).
[7]W.H. Matthaeus and D. Montgomery, Ann. N.Y. Acad. Sci. **357**, 203 (1980).
[8]A. Greco, P. Chuychai, W. H. Matthaeus, S. Servidio and P. Dmitruk, Intermittent MHD structures and classical discontinuities, Geophys. Res. Lett. **35**, L19111 (2008).
[9]Greco, A., Matthaeus, W. H., Servidio, S., Chuychai, P., and Dmitruk, P.: Statistical Analysis of Discontinuities in Solar Wind ACE Data and Comparison with Intermittent MHD Turbulence, ApJ **691**, L111 (2009).
[10]Wan, M., Oughton, S., Servidio, S., and Matthaeus, W. H.: Generation of non-Gaussian statistics and coherent structures in ideal magnetohydrodynamics, Phys. Plasmas **16**, 080703 (2009).
[11]C. Torrence, G.P. Compo, A practical guide to wavelet analysis. Bull. Am. Meteorol. Soc. **79**, 6178 (1998).
[12]A. Clauset, C. Rohilla Shalizi, M.E.J. Newman, Power-law distributions in empirical data, SIAM Rev. **51**, 661703 (2009).
[13]Frisch, U. 1995, *Turbulence* (Cambridge: Cambridge Univ. Press)
[14]M. Wan, K. T. Osman, W. H. Matthaeus, and S. Oughton, Investigation of intermittency in magnetohydrodynamics and solar wind turbulence: scale-dependent kurtosis, ApJ **744**, 171 (2012).
[15]Servidio, S., Greco, A., Matthaeus, W. H., Osman, K. T., and Dmitruk, P.: Statistical association of discontinuities and reconnection in magnetohydrodynamic turbulence, J. Geophys. Res. **116**, A09102 (2011).
[16]T. Gray, V. S. Lukin, M. R. Brown, C. D. Cothran, Three-dimensional reconnection and relaxation of merging spheromak plasmas, Phys. Plasmas **17**, 102106 (2010).

[17]Goldstein, M.L., Roberts, D.A. and Fitch, C.A. Jour. Geo. Res. **99** 11519-11538 (1994).
[18]Ji, H., Prager, S.C. and Sarff, J.S. Phys. Rev. Lett. **74** 2945 (1995).
[19]Telloini, D. *et al.*. ApJ. **751** 19 (2012).
[20]Matthaeus, W.H. and Velli, M. Space Sci. Rev. **160** 145-168 (2011).
[21]A. Greco *et al.* ApJ. **749** 105 (2012).